Supporting Information

Le et al. 10.1073/pnas.0914433107

SI Experimental Procedures

Cell Lines and Hypoxic Exposure. P493 human lymphoma B cells were maintained in RPMI 1640 with 10% (vol/vol) FBS and 1% (wt/vol) penicillin–streptomycin. P198 human pancreatic cancer cells, RCC4 and RCC4-VHL human renal carcinoma cells, and MCF-7 and MDA-MB-453 breast cancer cells were maintained in high-glucose (4.5 mg/mL) DMEM with 10% (vol/vol) FBS and 1% (wt/vol) penicillin–streptomycin. Nonhypoxic cells (20% (vol/vol) O_2) were maintained at 37 °C in a 5% (vol/vol) CO_2 and 95% (vol/vol) air incubator. Hypoxic cells (1% O_2) were maintained in a controlled atmosphere chamber (PLAS-LABS) with a gas mixture containing 1% O_2, 5% (vol/vol) CO_2, and 94% (vol/vol) N_2 at 37 °C for the indicated time. Bright live cells were counted daily in a hemacytometer using trypan blue dye to exclude dead cells. All cells were grown at a concentration of 10^5 cells /mL. All drug treatments began at day 0. FX11 was added daily.

RNA Interference Experiments. siRNAs targeting human LDHA (ON-TARGETplus SMARTpool) were purchased from Dharmacon Research, Inc. Targeting sequences for LDHA were a pool of the following four target sequences: sequence 1, GGAGAAAGCCGUCUUAAUU; sequence 2, GGCAAAGACUAUAAUGUAA; sequence 3, UAAGGGUCUUUACGGAAUA; and sequence 4, AAAGUCUUCUGAUGUCAUA. For P493 human lymphoma B cells, transfection of siRNAs was performed using an Amaxa Nucleotransfection device according to the manufacturer's instructions. Briefly, 2 μg of siLDHA ON-TARGETplus SMARTpool or ON-TARGETplus Nontargeting Pool (Dharmacon Research, Inc.) was transfected into 2×10^6 cells at 0 h. At 24 h, 10^5 cells were treated with 0.1% DMSO or FX11 for 48 more hours. The remaining cells were harvested for immunoblot analysis. For P198 human pancreatic cancer cells, transfection of siRNAs was performed using X-tremeGENE siRNA Transfection Reagent (Roche) according to the manufacturer's instructions.

Western Blot Analysis. Cell pellets were harvested after washing with PBS. Protein concentration was determined by BCA assay (Pierce) and 30 μg of protein per well was separated by SDS/PAGE and transferred by iBlot gel transfer stacks (Invitrogen). Rabbit monoclonal anti-LDHA (Epitomics) was used to detect human LDHA; phosphor-AMP kinase α and phospho-acetyl-CoA carboxylase antibodies were purchased from Cell Signaling. Membranes were reprobed with anti-α-tubulin as a loading control. The enhanced chemiluminescence reagent ECL (GE Healthcare) was used for detection.

Oxygen Consumption. Oxygen consumption was measured using a Clark-type oxygen electrode (Oxytherm System; Hansatech Instruments Ltd). Then, 5×10^6 cells in 1 mL of medium were placed in the chamber above a membrane that is permeable to oxygen. Oxygen diffuses through the membrane and is reduced at the cathode surface so that a current flows through the circuit, which is completed by a thin layer of KCl solution. The current that is generated bears a direct stoichiometric relation to the oxygen reduced and is converted to a digital signal. Determinations were done in triplicate, and the entire experiment was done twice.

ROS Measurement by Flow Cytometry. Intracellular ROS production was measured by staining cells with 5-(and-6)-carboxy-2′,7′-dichlorodihydrofluorescein diacetate (carboxy-H_2DCFDA; Molecular Probes) according to the manufacturer's instructions. Next, 10^5 cells/mL were treated with 9 μM FX11 or 0.5 nM FK866 for 24 h. Stained cells were analyzed in FACScan flow cytometers (BD Bioscience).

Annexin V Assay. After 24 h of FX11 treatment, cells were harvested and washed twice with cold PBS and the assay was performed using the Annexin V–7-AAD apoptosis detection Kit I (BD Biosciences Pharmingen) according to the manufacturer's instructions.

Determination of K_i and Enzyme Kinetics. The reaction velocity of purified human LDHA or GAPDH was determined by a decrease or increase, respectively, in absorbance at 340 nm of NADH. The LDHA activity was assessed using the protocol described in the *Worthington Enzyme Manual*, with varying concentrations of NADH. The GADPH activity was assessed using the protocol described in the *Worthington Enzyme Manual* with varying concentrations of NAD^+. K_i values were determined from double-reciprocal plots by linear regression analysis using SigmaPlot Enzyme Kinetic software.

CarboxyLink Immobilization and Affinity Columns. FX11 and E molecules that contain carboxyl groups were coupled to immobilized diaminodipropylamine resins according to the manufacturer's instructions (Pierce). About 1.9 mg (95% coupling efficiency) of FX11 or E was coupled to 2 mL of resin as estimated by the amount of either molecule recovered after conjugation. An equal amount of cell lysate was loaded onto these beads and eluted with 1 mM NADH after washing with six column volumes of high salt (1 M NaCl). LDHA activity was performed from the eluates to assess the binding affinity of the molecules with LDHA.

Mitochondrial Membrane Potential Measurement by Flow Cytometry. The lipophilic cation dye [JC-1(5,5′,6,6′-tetrachloro-1,1′,3,3′-tetraethylbenzimidazolcarbocyanine iodide); Invitrogen) was used to detect the loss of the mitochondrial membrane potential. The negative charge established by the intact mitochondrial membrane potential lets the lipophilic dye stain the mitochondria bright red, which emits in channel 2 (FL2). When the mitochondrial membrane potential collapses, JC-1 remains in the cytoplasm in a green fluorescent monomeric emission in channel 1 (FL1). JC-1 reversibly changes its color from green to orange as membrane potentials increase (over values of 80–100 mV). Then, 10^5 cells/mL were treated with 9 μM FX11 and/or FK866 for 24 h. Stained cells were analyzed in FACScan flow cytometers (BD Bioscience).

Measurement of ATP. P493 cells were treated with 9 μM FX11 or 0.5 nM FK866 for 20 h and counted. ATP levels were determined by a luciferin–luciferase-based assay (Promega) on aliquots containing equal number of cells according to a standard protocol.

Determination of NADH/NAD^+ and NADPH/$NADP^+$ Ratios. The NADH /NAD^+ and NADPH /$NADP^+$ ratios were assessed using the protocol described by the manufacturer. The assay is based on an enzyme-catalyzed kinetic reaction in which a tetrazolium dye 3-[4,5-dimethylthiazol-2-yl]-2,5-diphenyltetrazolium bromide is reduced by NAD(P)H in the presence of phenazine methosulfate. The intensity of the reduced product color, measured at 565 nm, is proportionate to the NAD(P)H /$NAD(P)^+$ concentration in the samples. The NAD(P)H or $NAD(P)^+$ content of the cells was harvested separately using a corresponding extraction buffer.

Visualization of NADH Autofluorescence and Emission Scanning. The NADH content of the cells was analyzed at an excitation wave length of 350 nm (UV) using an argon laser and was collected at 460 nm. The fluorescence emission spectrum of purified NADH, FX11, E, and FK866 was performed in a quartz cuvette with a 10-mm path length using a Quanta Master spectrofluorometer (Photon Technology International).

Measurement of Lactate Production. Lactate production was measured by the ABL700 Radiometer analyzer (Radiometer America, Inc.) according to the manufacturer's instructions. A total of 10^5 cells were grown at 37 °C in a 5% (vol/vol) CO_2 and 95% (vol/vol) air incubator and treated with 9 μM FX11 or 0.5 nM FK866 for 24 h.

Glucose Uptake Assay. A glucose uptake assay was performed using 2-[N-(7-nitrobenz-2-oxa-1,3-diazol-4-yl)amino]-2-deoxy-D-glucose (2-NBDG; Invitrogen) and a fluorescent analogue of 2-deoxyglucose, followed by flow cytometric detection of fluorescence produced by the cells. After 24 h, 10^5 cells/mL treated with 10 μM FX11 were incubated with 2-NBDG (100 μM) for 30 min. The 2-NBDG uptake reaction was stopped by removing the incubation medium and washing the cells with precold PBS. Vital dye 7-amino-actinomycin (7-AAD) was added to distinguish the viable cell population. For each measurement, data from 10,000 single-cell events were collected using FACScan flow cytometers (BD Bioscience).

Immunohistochemistry and Immunofluorescence Staining. Tumor and organ hypoxic areas were detected by pimonidazole hydrochloride (Hypoxyprobe) from Natural Pharmacia International. Hypoxyprobe (1.5 mg) diluted in 150 μL of 0.9% saline was given via i.p. injection 1 h before tumors were rapidly harvested and fixed in 10% (wt/vol) neutral formalin buffer. Aqua DePar and Bord Decloaker RTU (Biocare Medical) were used according to the two-step deparaffinization and heat retrieval protocol of the manufacturer. Protein adducts of reductively activated pimonidazole were detected by rabbit anti-Hypoxyprobe antibody. The immunohistochemical reaction was visualized by diaminobenzidine (Dako). The immunofluorescence reaction was visualized by Texas-red goat anti-rabbit antibody (Invitrogen). Samples were analyzed under an Axiovert 200 (Zeiss) fluorescence microscope at ×10 magnification.

Animal Studies. The animal studies were performed according to the protocols approved by the Animal Care and Use Committee at The Johns Hopkins University. To generate tumorigenesis study in xenograft model, 2.0×10^7 P493 human lymphoma B cells or 5×10^6 human pancreatic cancer cells were injected s.c. into male SCID mice (National Cancer Institute) or athymic Hsd: RH-Foxn1nu mice (Harlan), respectively, as previously described (1, 2). When the tumor volume reached 200 mm^3, groups of five mice were injected with control 2% (vol/vol) DMSO or 42 μg of FX11 and/or 100 μg of FK866. The tumor volumes were measured using digital calipers after 4, 7, and 10 days of treatment. Tumor volumes were calculated using the following formula: [length (mm) × width (mm) × width (mm) × 0.52]. The entire experiment was repeated seven times.

Statistical Analysis. The CI-50 was calculated using R 2.9.1 software (Bell Laboratories) by least-squares fitting of the data points using formulas shown here. Values are shown as mean ± SD or SEM. Data were analyzed by *t* test and confirmed by R 2.9.1 software. Significance was defined as $P < 0.05$.

Calculation of CI-50 for the Combination of FX11 and FK866. To estimate synergy, we fit cell count data gathered on day 2 to the following dose–response model:

$$\text{Count} = \text{Co}\{1 - \text{I}_{\text{max}}[\text{E1} + \text{E2} - (1 - \text{s})\text{E1E2}]\}$$

where Count is cell counts, Co is the estimated cell counts in the control case (without either drug); I_{max} is the maximum inhibition attainable on that day; E1 is the effect from drug 1 (FX11) alone [$E1 = D1/(IC50_1 + D1)$], E2 is the effect from drug 2 (FK866) alone [$E2 = D2/(IC50_2 + D2)$], s is a synergy parameter, and $IC50_1$ and $IC50_2$ are the amounts of drug 1 (D1 and D2) that yield 50% of their maximum inhibitory effect.

The fit was calculated using the nonlinear least squares library (3) in R (4) and yielded the following parameter estimates:

With these parameter values, we checked synergy via the "Loewe Additivity" (5), finding the drug fraction (f50) of each

Parameter	Estimate	SE	*P*
C_o	52.9	3.82	3.19e-13
I_{max}	0.743	0.0567	1.05e-12
$IC50_1$ (FX11)	4.56	1.77	0.017
$IC50_2$ (FK866)	0.00445	0.0019	0.027
s	0.252	0.112	0.033

drug's IC50 that, in combination together in the model, yields 50% of maximum inhibition:

$$\text{CI} - 50 = \text{f} + \text{f} = 0.78$$

This value of CI-50 is less than 1.0, the fraction of IC50 of a single drug that would achieve 50% of maximum inhibition. We therefore conclude that the two drugs are synergistic.

1. Feldmann G, et al. (2007) Blockade of hedgehog signaling inhibits pancreatic cancer invasion and metastases: A new paradigm for combination therapy in solid cancers. *Cancer Res* 67:2187–2196.
2. Gao P, et al. (2007) HIF-dependent antitumorigenic effect of antioxidants in vivo. *Cancer Cell* 12:230–238.
3. Bates DM and Chambers JM (1992) *in Statistical Models in S*, eds Chambers JM and Hastie JM (Wadsworth & Brooks/Cole, Belmont, CA), pp 421–454.
4. Ihaka R, Gentleman R (1996) R: A language for data analysis and graphics. *Journal of Computational and Graphical Statistics* 5:299–314.
5. Loewe S, Muischnek H (1926) Über Kombinationswirkungen. *Arch Exp Pathol Pharmakol* 114:313–326.

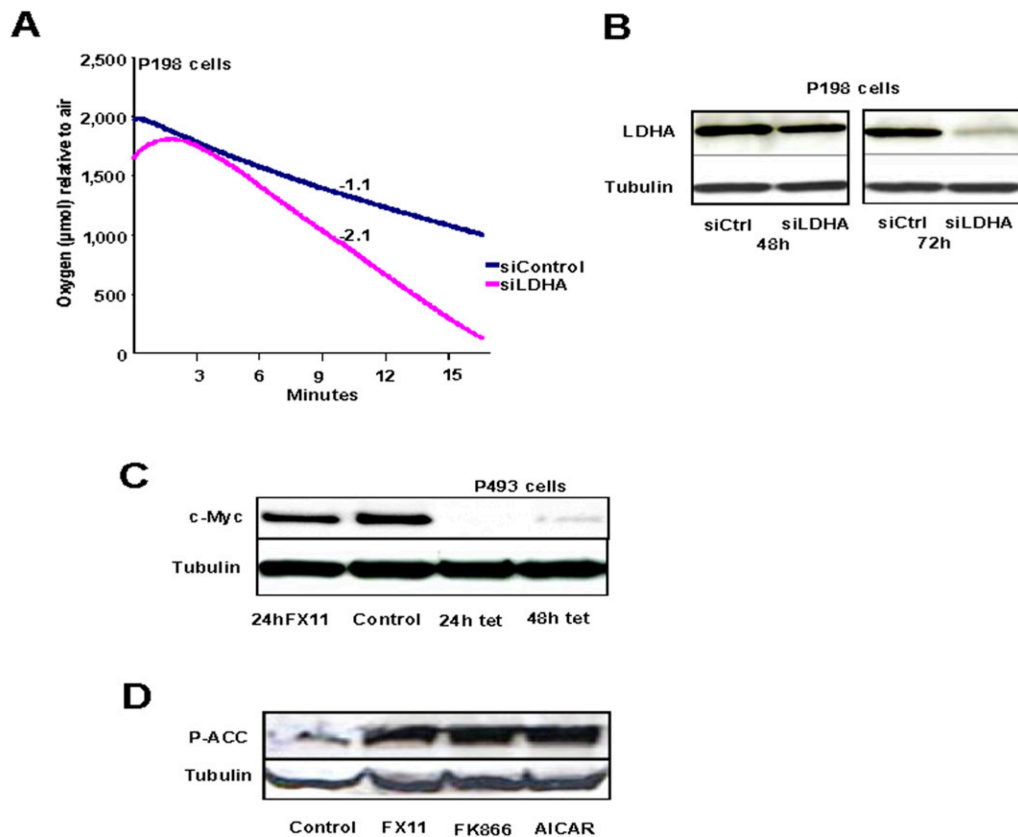

Fig. S1. (*A*) Effect of reduced LDHA expression by siRNA on oxygen consumption in P198 human pancreatic cancer cells. Oxygen consumption was determined by the use of a Clark-type oxygen electrode at 72 h posttransfection with siLDHA (slope = −2.1) or siControl (slope = −1.1). (*B*) Immunoblotting was performed on whole-cell lysates, probed with rabbit monoclonal anti-LDHA antibody, and reprobed with anti-α-tubulin as a loading control. (*C*) FX11 does not affect c-Myc levels in P493 cells. Tetracycline, known to repress c-Myc expression, was used as a control. Equivalent amounts of proteins were immunoblotted with anti-c-Myc antibody, and α-tubulin served as a loading control. (*D*) Activation of phospho-acetyl-CoA carboxylase (P-ACC) in lysates of cells treated with FX11 or FK866. Western blot analysis was performed after 24 h of treatment. Equivalent amounts of proteins were immunoblotted with anti-P-ACC, and α-tubulin served as a loading control.

Fig. S2. (*A* and *B*) FX11 and its derivative E are competitive inhibitors of LDHA with NADH as substrate. Lineweaver–Burk plots were determined from triplicate experiments using averages of activities. K_i determination was performed with 13.5 μM FX11 or 27 μM E. (*C*) Affinity chromatography of LDHA using sepharose-immobilized FX11 or E. Equal volumes of P493 human B cell lysates were chromatographed with six column volumes of high salt (1 M NaCl) wash, followed by elution with 1 mM NADH. LDHA activity was determined for each fraction, and the experiment was replicated with a representative experiment shown.

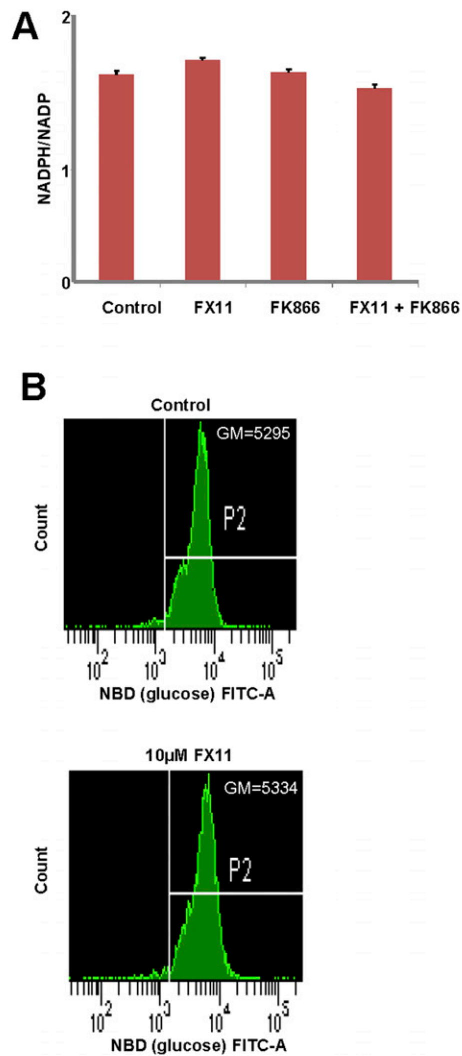

Fig. S3. (*A*) FX11 and/or FK866 effects on NADPH/NADP$^+$ ratio. P493 cells were treated with 10 μM FX11 and/or 0.1 nM FK866 for 24 h before the NADPH/NADP ratio was assayed. FX11 treatment compared with the control ($P = 0.8$) and FK866 treatment compared with the control ($P = 0.9$). (*B*) Effects of FX11 treatment on glucose uptake by P493 cells. A fluorescent analogue of 2-deoxyglucose (2-NBDG) was used to assay the glucose uptake of P493 cells, followed by flow cytometry. Viable cells taking up glucose were determined by negative 7-AAD and positive 2-NBDG. The number in each panel indicates the geometrical mean of green fluorescence intensity (520 nm) of the cell population.

Fig. S4. (*A*) Effect of FK866 and FX11 on P493-6 cell proliferation. Live cells were counted using trypan blue dye exclusion. Experiments were done in duplicate, and the entire experiment was repeated two times with similar results. The bars represent the averages of duplicate samples from one experiment. The combination of FX11 and FK866 doses revealed a CI-50 = 0.78 calculated using R 2.9.1 software. (*B*) FX11 treatment increases cellular NADH fluorescence of P493-6 cells compared with control, compound E, or FK866 treatment. The number in the P2 box represents the average percentage of cellular NADH autofluorescence ($n = 3$). FX11 treatment compared with control ($P = 0.005$), FK866 compared with control ($P = 0.144$), and E treatment compared with control ($P = 0.38$). (*C*) Fluorescence emission spectrum of NADH (green line), FX11 (red line), or E (blue line). Note that the emission maxima of FX11 or E (390 nm) do not coincide with that of NADH (460 nm), excluding the direct contribution of FX11 to the autofluorescence of FX11-treated cells at 460 nm.

Fig. S5. (*A–D*) RCC4 cells and MCF-7 cells are more sensitive to FX11 than RCC4-VHL and MDA-MB-453 cells. Cell population growth of human renal carcinoma RCC4 and RCC4-VHL cells or human breast cancer MCF-7 and MDA-453 cells in response to different doses of FX11. (*E*) Effect of FX11 on the proliferation of P493 cells is glucose-dependent. Cell population growth of P493 cells in the absence of glucose and in the presence or absence of 9 μM FX11. (*F*) LDHA-dependent effect of FX11. Cell population growth of P493 cells with siRNA-mediated reduced LDHA expression in the presence or absence of 9 μM FX11. Cell numbers are shown as mean ± SD.

PNAS PNAS PNAS

Fig. S6. (*A* and *B*) Characterization of glucose, glutamine, and pyruvate dependency of different human breast cancer cell lines, MCF-7 and MDA-MB-453. Cells were cultured in media with different availability of glucose, glutamine, and pyruvate. All media were supplemented with 10% (vol/vol) bovine fetal serum and 1% penicillin–streptomycin. Averages of cell numbers from triplicate experiments are shown ± SD. (*C*) Growth curves for control, electroporated, and siControl cells compared with cells treated with siLDHA. ON-TARGETplus pool was used as siRNAs targeting human LDHA, and Nontargeting Pool was used as siControl. The siRNAs were transfected into 2×10^6 cells at 0 and 24 h by electroporation. (*D*) Cells were harvested for immunoblot analysis. Rabbit monoclonal anti-LDHA was used to detect LDHA, and the membrane was reprobed with anti-α-tubulin as a loading control.

Fig. S7. Hypoxia accentuates the sensitivity of human P493 B cells (*A* and *B*) and human P198 pancreatic cancer (*C* and *D*) cells to FX11 inhibition of growth. Cell population growth of P493 B cells or pancreatic cancer P198 cells in normoxia or hypoxia with different doses of FX11. Normoxic cells were grown at 37 °C in a 5% (vol/vol) CO_2 and 95% (vol/vol) air incubator. Hypoxic cells (1% O_2) were maintained for the indicated time in a controlled atmosphere chamber with a gas mixture containing 1% O_2, 5% (vol/vol) CO_2, and 94% (vol/vol) N_2 at 37 °C. There is no significant difference in cell numbers between the 0% and 0.1% DMSO groups.

Fig. S8. (*A*) Pimonidazole-labeling of hypoxic regions (dark brown) of spleen, liver, and P493-6 lymphoma. (*B*) FX11 treatment diminishes hypoxic regions of P493 lymphoma. Rabbit anti-Hypoxyprobe antibody was used as the primary antibody. Texas-red anti-rabbit and DakoCytomation EnVision+ System-HRP anti-Rabbit antibody were used as secondary antibodies for immunofluorescence and immunohistochemistry, respectively. Samples were analyzed under an Axiovert 200 (Zeiss) fluorescence microscope at ×0 magnification. Ten random fields from an untreated tumor and a treated tumor were photographed. (*C*) Effect of FX11 treatment vs. vehicle control on LZ10.7 human pancreatic cancer xenografts ($P = 0.03$). A total of 5×10^6 LZ10.7 cells were injected s.c. into athymic nude mice. When the tumor volume reaches 150 mm^3, 42 μg of FX11 or DMSO, which is used as vehicle control, was injected i.p. daily and observed for 10 days. The tumor volumes were measured using digital calipers and calculated using the following formula: [length (mm) × width (mm) × width (mm) × 0.52]. The results represent the average ± SEM.

Fig. S9. Effect of FX11 treatment on blood chemistries and hematology. Average values ± SD are shown for five animals in each group. ALB, albumin; ALP, alkaline phosphatase; ALT, alanine aminotransferase; AMYL, amylase; AST, aspartate aminotransferase; BA, basophils; CAL, calcium; Chol, cholesterol; CL, chloride; CREAT, creatinine; EO, eosinophils; GLU, glucose; HB, hemoglobin; HCT, hematocrit; K, potassium; LY, lymphocytes; MCH, mean corpuscular hemoglobin; MCHC, mean corpuscular hemoglobin concentration; MCV, mean corpuscular volume; MO, monocytes; NA, sodium; NE, neutrophils; RBC, red blood cells; RDW, red cell distribution width; TBILI, total bilirubin; TPROT, total protein; Tri, triglyceride; UA, uric acid; WBC, white blood cells.